Contact induced magnetism in carbon nanotubes

2004 J. Phys.: Condens. Matter 16 L155

(http://iopscience.iop.org/0953-8984/16/10/L06)

INSTITUTE OF PHYSICS PUBLISHING JOURNAL OF PHYSICS: CONDENSED MATTER

J. Phys.: Condens. Matter **16** (2004) L155–L161 PII: S0953-8984(04)76015-4

LETTER TO THE EDITOR

Contact induced magnetism in carbon nanotubes

O Céspedes[1], M S Ferreira, S Sanvito, M Kociak[2] and J M D Coey

Physics Department, Trinity College, Dublin 2, Republic of Ireland

E-mail: cespedeo@tcd.ie

Received 4 February 2004
Published 27 February 2004
Online at stacks.iop.org/JPhysCM/16/L155 (DOI: 10.1088/0953-8984/16/10/L06)

Abstract

Evidence is presented to show that carbon nanotubes can become magnetized when they are in contact with magnetic material. Spin-polarized charge transfer at the interface between a flat ferromagnetic metal substrate and a multiwalled carbon nanotube leads to a spin transfer of about 0.1 μ_B per contact carbon atom. The corresponding magnetization is detected by using magnetic force microscopy to probe the stray field in the neighbourhood of the nanotube. Magnetic contrast is observed for carbon nanotubes placed on cobalt or magnetite substrates, but it is absent on silicon, copper or gold substrates. This observation of contact-induced magnetism opens a new avenue for implementing spin-electronics at the molecular level, where the current leads can be separated from the electrodes producing spin polarization.

(Some figures in this article are in colour only in the electronic version)

There are recurrent reports that graphite [1] and other forms of carbon [2–4] can exhibit a weak ferromagnetic moment, which persists well above room temperature. An explanation in terms of bond defects or impurities is usually proposed [3–5]. Studies of magnetic carbon report moments per unit mass ranging from $\sigma = 10^{-3}$ up to 20 A m^2 kg^{-1} [4], values that are put in perspective by comparing with the 465 A m^2 kg^{-1} that is equivalent to a graphite moment of 1 μ_B per carbon atom. The graphite magnetization corresponding to 1 μ_B/C is $M = 1020$ kA m^{-1}.[3] The weakness and variability of these moments, together with the question of whether samples are ever completely pure, clouds the significance of the measurements. The magnetization distribution may be inhomogeneous [3, 5], and can sometimes be related to specific defects [5]. Common magnetic impurities such as iron ($\sigma = 220$ A m^2 kg^{-1}) and magnetite ($\sigma = 80$ A m^2 kg^{-1}) may play a role.

[1] Author to whom any correspondence should be addressed.

[2] Present address: Laboratoire de Physique des Solides, Bâtiment 510, porte 232, Université Paris-Sud, 91405 Orsay, France.

[3] cgs conversion: magnetic moment per unit mass σ:1 A m^2 kg^{-1} = 1 emu g^{-1}; magnetic moment per unit volume M:1 kA m^{-1} = 1 emu cm^{-3} ($4\pi M$); magnetic field H:1 kA m^{-1} = 12.6 Oe.

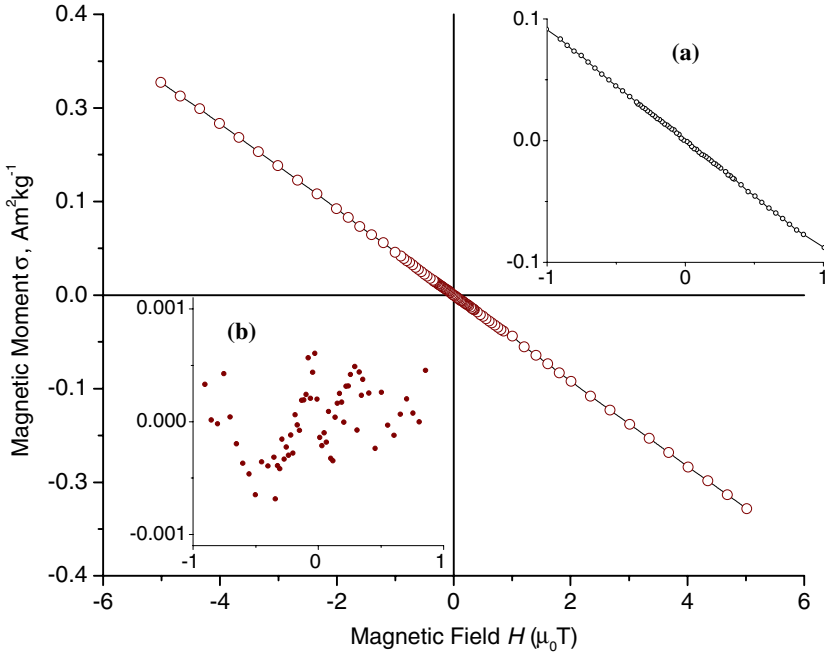

Figure 1. Susceptibility of the multiwalled carbon nanotubes measured at room temperature using a SQUID magnetometer. Inset (a) shows the susceptibility in low field. Inset (b) shows the magnetic moment per unit mass once the diamagnetic contribution is subtracted. Transition metal impurities measured by inductively coupled plasma (ICP) are below the detection limit of 1 ppm. Any ferromagnetic moment of the tubes is less than 5×10^{-4} A m^2 kg^{-1}, corresponding to a magnetization $M < 0.001$ kA m^{-1}.

A recent examination of samples of a graphite nodule from the Canyon Diablo meteorite [6] concluded that there was a residual magnetization corresponding to a moment $m \approx 0.05\,\mu_B$/C, which was unexplained by the magnetic phases present in the nodule. It was suggested that the ferromagnetism was due to a magnetic proximity effect induced at the interfaces of graphite with nanoscale magnetite or kamacite ($Fe_{93}Ni_7$) inclusions. We therefore set out to find direct experimental evidence of contact-induced magnetism, and gain some understanding of its origin. Our idea was to place a carbon nanotube in contact with a ferromagnet and measure the spin transfer associated with the alignment of their chemical potentials. The problem of detecting the tiny spin transfer against the huge background magnetic moment of the ferromagnet was resolved by taking a smooth ferromagnetic thin film as a substrate and looking for a stray field around the nanotube. Uniformly magnetized thin films create no stray field, whatever their direction of magnetization. Therefore any observed stray field must arise from the tube. Cobalt and magnetite were chosen as magnetic substrates; Co because it forms a rather strong chemical bond involving $3d_{z^2}$ and graphite p_z electrons, and Fe_3O_4 because it is a half-metal with a high magnetic ordering temperature (860 K), where the spin transfer should be equal to the charge transfer. Si, Cu and Au substrates are used for control purposes.

The nanotubes are ropes composed of several multiwalled strands, obtained by arc discharge [7]; they were chosen for ease of imaging and freedom from ferromagnetic impurities. The diamagnetic susceptibility is $\chi = -8 \times 10^{-8}$ m^3 kg^{-1} (figure 1). Other types of nanotube are unsuitable because they are prepared using a catalyst of iron or cobalt, which contaminates the carbon.

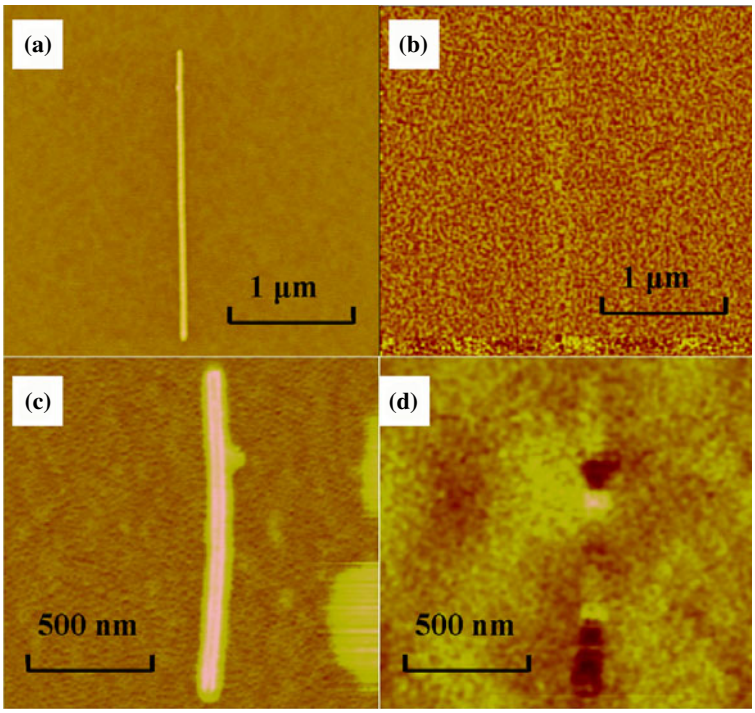

Figure 2. (a) Atomic force micrograph (AFM) of a multiwalled carbon nanotube laid on a Si substrate and (b) magnetic force micrograph (MFM) of the same tube; the scale is 0.4 °. (c) AFM of another tube on a Co substrate and (d) MFM of the same tube; the scale is 0.8°. In all the MFMs, the amplitude of oscillation was chosen to be as close to the lift height as possible without touching the sample.

Tubes were placed on the different substrates, and topographic and magnetic images were recorded by atomic and magnetic force microscopy (AFM/MFM) at room temperature using a 'Nanoscope III' instrument. The magnetic information was obtained in the lift mode with permalloy or Co–Cr coated tips (which have a permanent magnetic moment) using amplitude or phase detection, respectively. A typical AFM image of a tube laid on a silicon substrate is shown in figure 2(a); the corresponding MFM image in figure 2(b) is featureless; the tube is nonmagnetic and produces no stray field. Similar null results are obtained on gold or copper substrates, provided the lift height is sufficient to avoid ghost images.

The images on cobalt or magnetite substrates are quite different. The topographic image on a sputtered cobalt film 60 nm thick with a mean surface roughness of 0.35 nm is similar to the previous one (figure 2(c)) but now there is magnetic contrast (figure 2(d)).

We have performed hundreds of measurements and found many images where a stray field is coming from the tube, provided the substrate is magnetic. Approximately 20% of all tubes placed on magnetic substrates exhibited contrast in their magnetic images. The stray field from the nanotube is usually unrelated to any stray field arising from the substrate because of multidomain structure or surface roughness. In figure 3(a) magnetic contrast is shown for a sample lying on a flat cobalt substrate that has been magnetized and generates no discernible contrast. Figure 3(b) on the other hand, shows a nanotube on top of a non-uniformly magnetized Co film, which itself produces some magnetic contrast, but additional contrast due to the tube is visible. In figure 3(c), there is a much stronger signal from the cobalt film, which has

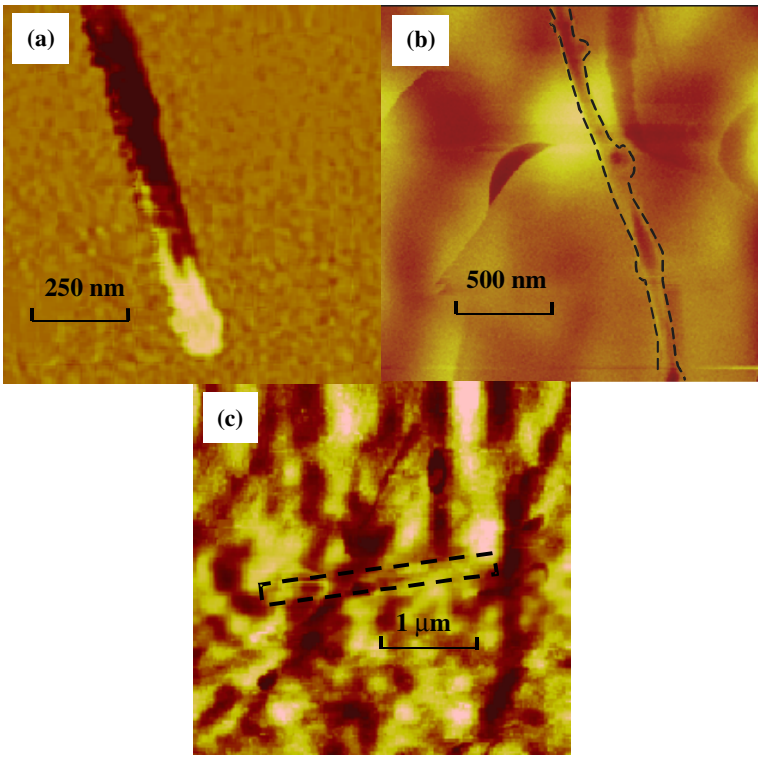

Figure 3. Magnetic force micrographs of multiwalled nanotubes on different cobalt substrates obtained with a Co–Cr coated tip in the phase mode at lift heights in the range 40–70 nm. (a) The edge of a rope composed of two or three tubes on a uniformly magnetized Co substrate (the vertical scale is 0.5°), where the magnetic force micrograph shows magnetic contrast between and along the tubes. Panel (b) shows another tube on a Co substrate which itself shows weak magnetic contrast, but that in the tube is different from that of the substrate (1° scale). Panel (c) shows a substrate with strong magnetic contrast (3° scale) to which the tube is essentially transparent.

been deposited on a polycrystalline ruthenium seed layer, and the tube makes no perceptible contribution to the strong magnetic contrast provided by the substrate.

Figure 4 shows some images of a carbon nanotube on Fe_3O_4 taken at different scan heights. The magnetic images in figures 4(a) and (b) show little contrast to the magnetite substrate, and clear bipolar contrast to the nanotube, as expected if it were a single domain magnetized along its length. These images suggest that the tube is aligned with the direction of magnetization of a single, in-plane domain in the substrate. Shape anisotropy of the film ensures that its magnetization lies in-plane, and any weak stray field comes from surface irregularity, ripple domains or Bloch walls. The images in figures 4(c) and (d) are of the same tube in a slightly different position.

The data in figure 4 indicate that the magnetic contrast depends weakly on lift height in the range from 40 to 120 nm. In practice, the signal phase $\Delta\varphi$ is roughly constant at close tip–sample separations [8]. For example, when magnetic fields are generated by passing a current through a single turn of a coil of radius r, it has been observed that $\Delta\varphi$ varies as $(1 - l/r)$ for distances $< r$, where l is the lift height [9]. At low lift, the magnetic field of up to 30 kA m^{-1} generated by the tip can interact with the tube or the substrate [10], or the tip itself can even change the position of the nanotube.

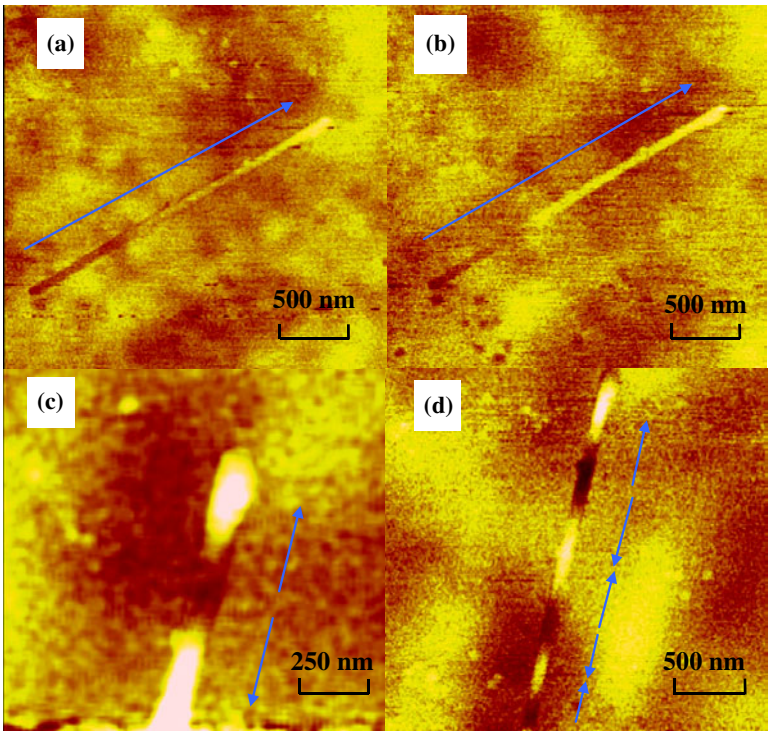

Figure 4. Magnetic force micrographs of a multiwalled nanotube lying on a magnetite substrate obtained in the amplitude mode with a low moment, permalloy-coated tip. (a) Scan at 60 nm lift (the scale is 60 mV), (b) scan at 90 nm lift (scale 40 mV); the tube shows a single domain configuration magnetized along its length. In (c) and (d) scans of the same tube in a slightly different position are shown at 40 nm (c) and 120 nm (d) lift with a scan direction at 45° with respect to that used for (a) and (b); the scale is 40 mV for both pictures. The original dipole configuration has split into several domains.

In order to estimate the magnitude of the induced magnetization of the carbon nanotube, we compared our images with those obtained from hard and floppy disks. From bits of 1 μm $\times$ 10 μm recorded on γ-Fe_2O_3, we obtain signals that are approximately one order of magnitude greater than those from the carbon nanotubes. The medium has magnetization $M \approx 200$ kA m^{-1}, and it produces a stray field of the order of 2 kA m^{-1} around each bit [11]. The dimensions of the recorded bits and nanotubes are similar, so the stray field gradients are expected to scale similarly. The weak dependence on lift height allows us to compare the stray fields generated by the tubes and the bits. The stray field close to the tube will be of the order of $0.2M$ if it behaves like a bar magnet, so we estimate a tube magnetization of the order of 1 kA m^{-1}, corresponding to an average carbon moment of the order of 0.001 μ_B. Finally, allowing for the fact that no more than 1% of the carbon atoms are likely to be in contact with the substrate, the observed magnetization corresponds to a moment of the order of 0.1 μ_B per contact atom.

The charge transfer for a (5, 5) carbon nanotube on a Au(111) surface was calculated as 0.1 electrons per contact carbon atom [12]. When the densities of states for spin up ($\uparrow$) and spin down ($\downarrow$) electrons at the Fermi level of the metal substrate are quite different, we expect a similar degree of spin transfer.

This has been analysed by assuming that the electronic structure of both the magnetic and non-magnetic material can be accurately described by a single-particle Hamiltonian, and that

the non-magnet has a hollow cylindrical structure atomically commensurate with the magnetic surface on which it lies. The change in density of states upon the band formation is written in terms of the separate single-particle Green functions for the isolated nanotube and the magnetic surface. Our central results [13] are two expressions, one for the spin dependent charge transfer to the nanotube:

$$\Delta N_{\mathrm{T}}^{\sigma} = \mathrm{Tr}\left\{\rho_{\mathrm{M}}^{\sigma}(E_{\mathrm{F}})[V_{\mathrm{T}}(E_{\mathrm{F}}) - \langle V_{\mathrm{T}}\rangle] + \rho_{\mathrm{T}}(E_{\mathrm{F}})[V_{\mathrm{M}}^{\sigma}(E_{\mathrm{F}}) - \langle V_{\mathrm{M}}^{\sigma}\rangle]\right\}, \tag{1}$$

and the other for the energy cost associated with the transfer:

$$\Delta E = \sum_{\sigma} \mathrm{Tr}[N_{\mathrm{M}}^{\sigma}\langle V_{\mathrm{T}}\rangle + N_{\mathrm{T}}\langle V_{\mathrm{M}}^{\sigma}\rangle]. \tag{2}$$

Here $\rho_i^{\sigma}(E_{\mathrm{F}})$ and N_i^{σ} are the spin-σ ($\sigma = \uparrow, \downarrow$) densities of states at the Fermi level and the total number of electrons, respectively; $i = \mathrm{T}$ refers to the tube and $i = \mathrm{M}$ to the substrate. $V_i^{\sigma}(E)$ are the energy-dependent contact potentials produced by the tube on the substrate ($i = \mathrm{T}$) and by the substrate on the tube ($i = \mathrm{M}$), and $\langle V_i^{\sigma}\rangle$ are averages over the relevant bandwidth. All these quantities, which can be accurately calculated, are matrices in the space of the relevant orbitals; the trace is taken over all the orbitals. ΔE in equation (2) must be negative for the spin and charge transfer to occur. The induced magnetization is the net spin imbalance of the electrons transferred to the nanotube $M = (\Delta N_{\mathrm{T}}^{\uparrow} - \Delta N_{\mathrm{T}}^{\downarrow})\,\mu_{\mathrm{B}}$. The contact potential $V_i^{\sigma}(E) = t\,\mathrm{Re}[\mathbf{G}_i^{\sigma}]t^{+}$, where $\mathbf{G}_i^{\sigma}$ is the single particle Green function and t is the coupling matrix between the substrate and the tube. Here t parameterizes the interaction between the two materials. In practice it is the hopping integral between the orbitals that is responsible for the chemical bonding. Magnetism is induced not just because we have a magnetic substrate, but also because the spin-polarized orbitals contribute to the chemical bond. Charge transfer, induced magnetic moment and energy cost all depend *quadratically* on t, which therefore sets both the size of the magnetic moment and the relevant energy scale.

Specifically we consider an (8, 8) armchair nanotube described by a single-band tight-binding model with hopping parameter $\gamma = 2.5$ eV where 6γ is the width of the graphite π-band [15], in contact with a magnetic transition metal with a 5 eV wide spin-polarized d band which is assumed to be orbitally degenerate. We take t to be the p-dσ hopping parameter between Co and C based on a density functional calculation for a Co/C superlattice, evaluating $t = V_{\mathrm{pd}\sigma} = 0.45$ eV by using Harrison's scaling law [14] with a Co–C band length of 2.72 Å. This gives magnetic moments $m \approx 0.1\ \mu_{\mathrm{B}}$ per contact carbon atom, and energy gains per unit cell $\Delta E \approx 0.1$ eV. These results confirm that the induced magnetic moment in the carbon nanotube should be observable at room temperature.

The magnetic proximity effect described here is quite distinct from spin-injection. Magnetic proximity produces an equilibrium spin imbalance in a non-magnetic material very close to its contact surface with a magnetic one, on the scale of the screening length, which in nanotubes may be approximately one nanometre. Spin-injection is a non-equilibrium spin imbalance of a transport current far from the contacts. The spin diffusion length in carbon nanotubes may be comparable to their length.

In conclusion, we have direct evidence for contact-induced magnetism due to spin-polarized charge transfer at a contact between a ferromagnet and a carbon nanotube. Although it is difficult to extract quantitative information from MFM images, the data are consistent with a spin transfer of the order of $0.1\ \mu_{\mathrm{B}}$ per contact carbon atom, and an induced magnetization of the order of 1 kA m^{-1} in multiwalled nanotubes. Controllable high-temperature ferromagnetism in graphite or carbon nanotubes is a tantalizing prospect because of the possibility of combining spin physics [15] with molecular electronics [16]. Graphitic structures have several crucial properties for spin and molecular electronics, such as a low effective mass and a long spin diffusion length exceeding 130 nm [17]. Moreover carbon nanotube electronic architectures,

such as logic circuits [18–20] and non-volatile random access memories have been already demonstrated [21]. The addition of the spin degree of freedom to this already rich physics can open new perspectives for spin-based high-speed devices, where logic and memory elements are integrated at the molecular level. Our results indicate that spin and charge functionalities can be integrated, while separating the charge contacts from those producing spin polarization by exploiting interface reflection for example.

This work was supported by Science Foundation Ireland. We are grateful to E Kerr and S Watts for providing the cobalt and magnetite films, and P Stamenov the SQUID measurements.

References

[1] Esquinazi P *et al* 2002 *Phys. Rev.* B **66** 024429
[2] Makarova T L *et al* 2001 *Nature* **413** 716–8
[3] Han K-H *et al* 2003 *Carbon* **41** 785
[4] Makarova T L 2003 Magnetism of carbon-based materials *Studies of High Temperature Superconductors* vol 45, ed A Narlikar (Hauppauge, NY: Nova Science Publishers) p 107
[5] Esquinazi P *et al* 2003 *Phys. Rev. Lett.* **91** 227201
[6] Coey J M D, Venkatesan M, Fitzgerald C B, Douvalis A P and Sanders I S 2002 *Nature* **420** 156
[7] Kwon Y-K, Saito S and Tománek D 1998 *Phys. Rev.* B **58** R16001
[8] Yongsunthon R *et al* 2002 *J. Appl. Phys.* **92** 1256
[9] Lohau J, Kirsch S, Carl A, Dumpich G and Wassermann E F 1999 *J. Appl. Phys.* **86** 3410
[10] McVitie S, Ferrier R P, Scott J, White G S and Gallagher A 2001 *J. Appl. Phys.* **89** 3656
[11] O'Handley R C 2000 *Modern Magnetic Materials* (New York: Wiley) pp 681–3
[12] Rubio A, Sanchez-Portal D, Artacho E, Ordejon P and Soler J M 1999 *Phys. Rev. Lett.* **82** 3520
[13] Ferreira M S and Sanvito S 2004 *Phys. Rev.* B **69** 035407
[14] Harrison W A 1980 *Electronic Structure and the Properties of Solids* (New York: Dover)
[15] Wolf S A *et al* 2001 *Science* **294** 1488
[16] Joachin C, Gimzewski J K and Aviram A 2000 *Nature* **408** 541
[17] Tsukagoshi K, Alphenaar B W and Ago H 1999 *Nature* **401** 572
[18] Bachtold A, Hadley P, Nakanishi T and Dekker C 2001 *Science* **294** 1317
[19] Huang Y *et al* 2001 *Science* **294** 1313
[20] Collins P G, Arnold M S and Avouris P 2001 *Science* **292** 706
[21] Rueckes T *et al* 2000 *Science* **289** 94